Journal of Nuclear Medicine, published on December 13, 2019 as doi:10.2967/jnumed.119.236893

^{18}F-fluorodexyglucose Position Emission Tomography identifies altered brain metabolism in patients with Cri du Chat syndrome

running title: brain PET in Cri du Chat Syndrome

The authors report no conflicts of interest.

Angelina Cistaro[1,2,3], Natale Quartuccio[2,4], Arnoldo Piccardo[1,2], Piercarlo Fania[5], Marianna Spunton[3,6], Alexandra Liava[3,7], Cesare Danesino[3,8], Giovanni Albani[3,9] and Andrea Guala[3,6]

1. Nuclear Medicine Department, Ente Ospedaliero Ospedali Galliera, Genoa, Italy
2. AIMN Pediatric Study Group
3. Scientific Committee of A.B.C. Associazione Nazionale Bambini Cri du Chat, Italy
4. Nuclear Medicine Unit, A.R.N.A.S. Ospedali Civico, Di Cristina e Benfratelli, Palermo, Italy
5. Independent Data Scientist, Turin, Italy
6. Paediatric Unit , Castelli Hospital, Verbania, Italy
7. Child Neuropsychiatric Unit, Castelli Hospital, Verbania, Italy
8.Department of Molecular Medicine, IRCCS Policlinico San Matteo, University of Pavia, Pavia, Italy.
9. Department of Neurology, Istituto Auxologico Italiano, IRCCS, Piancavallo-Verbania, Italy

Corresponding author:

Angelina Cistaro, MD
ORCID: 0000-0001-8024-8425
Nuclear Medicine Department, Ente Ospedaliero Ospedali Galliera, Genoa, Italy
Mura delle Cappuccine, 14, 16128 Genova GE
Phone number: +393288468333
Fax: +390916662315
Email: angelinacistaro06@gmail.com

Word count: 4515

The work has received financial support by "Associazione Bambini Cri du Chat".

ABSTRACT

Cri-Du-Chat Syndrome (CdCs) is a rare genetic disease caused by a deletion in the short arm of chromosome 5 (5p) with a variable clinical spectrum. To date no study in literature has ever investigated the alterations of brain glucose metabolism in these subjects by means of ^{18}F-fluoro-2-deoxy-d-glucose Positron Emission Tomography/Computed Tomography (^{18}F-FDG PET/CT). The aims of this study were to detect difference in brain ^{18}F-FDG metabolism in patients affected by CdCs with different clinical presentations and identify possible "brain metabolic phenotypes" of this syndrome. **Methods:** 6 patients (age: 5 M and 1 F, age range: 10-27) with CdCs were assessed for presence of cognitive and behavioral symptoms with a battery of neuropsychological tests and then classified as patient with a severe or mild phenotype. Then, patients underwent a brain ^{18}F-FDG PET/CT scan. PET/CT findings were compared to a control group, matched for age and sex, by using statistical parametric mapping (SPM). Association of different clinical phenotypes and ^{18}F-FDG PET/CT findings was investigated. **Results:** Four patients presented a severe phenotype, whereas 2 patients demonstrated mild phenotype. SPM single subject and group analysis compared to the control cohort revealed a significant hypometabolism in the left temporal lobe (BAs 20, 36 and 38), in the right frontal subcallosal gyrus (BA 34) and caudate body, and in the cerebellar tonsils ($p<0.001$). Hypermetabolism ($p=0.001$) was revealed in the right superior and precentral frontal gyrus (BA 6) in patient group compared to the control cohort. In SPM single subject analysis the hypermetabolic areas were detected only in patients with a severe phenotype. **Conclusions**: This study revealed different patterns of brain glucose metabolism in patients with severe and mild phenotype compared to control subjects. In particular, the hypermetabolic abnormalities in the brain, evaluated by^{18}F-FDG PET/CT, seem to correlate with the severe phenotype in patients with CdCs.

Key words: Cri-Du-Chat Syndrome, ^{18}F-FDG PET/CT, Statistical Parametric Mapping, Brain; Hypometabolism

INTRODUCTION

Cri-du chat syndrome (CdCs) is a rare genetic disease, with an incidence ranging from 1/15.000 to 50.000 live births, caused by either a partial or complete deletion of chromosome 5p (*1*). Clinical phenotype depends on the location and extension of the genomic region involved in the 5p deletion, with breakpoints localization varying from p13 (D5S763) to p15.2 (D5S18) (*2-5*), and it is characterized by different degree of severity of the developmental and behavioral problems. Physical and behavioral characteristics include high-pitched cry, microcephaly, broad nasal bridge, epicanthal folds, micrognathia, and severe psychomotor retardation (*2*). Diagnosis is based on clinical manifestations and requires karyotype, array comparative genomic hybridization and, eventually, fluorescence *in situ* hybridization for doubtful cases (*1,2*). The most frequent structural brain abnormalities, as shown by few studies available in literature using Magnetic Resonance Imaging (MRI), include brain stem hypoplasia (with predominant pontine involvement), thinning or agenesis of the corpus callosum, cerebellar vermian atrophy (or agenesis), cerebellar cortical thickening and incomplete arborization of white matter (*6,7*).

It is well established that ^{18}F-fluoro-2-deoxy-d-glucose Positron Emission Tomography/ Computed Tomography (^{18}F-FDG PET/CT) is an important tool for the assessment of cerebral metabolism in several neurological diseases, showing different metabolic patterns that support both an early diagnosis and a neurological disability evaluation (*8-10*). No study has ever correlated brain glucose metabolism with phenotypical presentation in patients with CdCs. Therefore, we aimed to investigate the brain glucose metabolism distribution in patients with CdCs and to identify possible "brain metabolic phenotypes" of this syndrome.

MATERIALS AND METHODS

We prospectively and consecutively evaluated 6 patients (1 female and 5 male, age range: 10-27) with CdCs, presenting different deletion size of the 5p region. Patients n. 5 and n. 6 were monozygotic twins with mosaic 46,XY,del(5)(p14)/46,XY. All six patients underwent a complete neurological and neuropsychiatric clinical assessment including Vineland adaptive behavior scales. According to the various levels of severity deficits in intellectual functions and adaptive functioning, as defined in DSM V (Diagnostic and Statistical Manual of Mental Disorders, fifth edition)(*11*), the patients were classified having mild and severe clinical phenotype.

Exclusion criteria were: 1) pregnancy; 2) inability to lie still for the duration of the PET scan (15 minutes); 3) presence of previous diagnosis of oncological or other neurological disease in the medical history.

The study was proposed by the Scientific Committee and approved by the Ethical Review Board (ERB) of the ABC (Associazione Bambini Cri du Chat). Each patient, or parents for patients less than 18 years old involved in the study, provided written informed consent after receiving a detailed description of the study's aims.

^{18}F-FDG Brain PET/CT Scanning

All brain PET/CT scans were performed after fasting for at least 6h and measurement of blood glucose level (max 130 mg/dl). Patients were positioned comfortably in a quiet and darkened lit room at least 20 min before ^{18}F-FDG administration and during the uptake phase of the radiopharmaceutical. They received intravenous injection of a fixed activity (185 MBq) of ^{18}F-FDG through an intravenous cannula according to EANM procedural guidelines (*12*). The PET/CT scans started approximately 60 min after injection and lasted 15 min. A polycarbonate head holder was applied to avoid head movements during the scan. The PET scans were acquired using a Discovery STE PET/CT System (General Electrics Medical Systems, Milwaukee, WI) in 3D modality with a total axial field of view of 30 cm and no interplane gap space. ^{18}F-FDG-PET/CT brain data were collected through sequential scans: CT data were used for the attenuation correction of the PET data, with thickness of 3.75 millimetres, 140kVolt, 60-80 mA/sec and PET brain scan with 1 FOV of 30 transaxial centimetres. PET data were reconstructed using a 3D-OSEM reconstruction iterative process algorithm with the corrections for random, scatter and attenuation (VUE-point). The parameters for the VUE-point were: number of subsets 28; number of iteration 4. Data were collected in 128×128 matrices with a reconstructed voxel of 1.33 x 1.33 x 2.00 mm.

Statistical Analysis

CdC-patient-group and CdC-single-subject analyses was performed comparing the ^{18}F FDG-PET brain scan with a neurologically normal group of healthy subjects, matched for age and sex, extracted from a control cohort of 40 healthy individuals, previously used in another research study (*13*). Preprocessing and statistical analyses were performed by statistical parametric mapping (SPM2, Wellcome Department of Cognitive Neurology, London, UK) implemented in Matlab 7.9 (Mathworks, Natick, MA). The spatially normalized set of images was smoothed using an 8-mm isotropic gaussian filter. The resulting statistical parametric maps, SPM{tdc}, were transformed into normal distribution (SPM{*z*}) units. The SPM coordinates were corrected to match the Talairach coordinates by the subroutine implemented by Matthew Brett (http://brainmap.org/index.html). Brodmann areas (BAs) were then identified at a range of 0 to 3 mm from the corrected Talairach coordinates of the SPM output isocentres, after importing the corrected coordinates, by Talairach client (http://www.talairach.org/index.html) performed using the SPM. To test the overall statistical significance of metabolic differences, one-way analysis of variance (ANOVA) was performed using the SPM2 f-contrast routine between CdC patient and control group. A two-sample unpaired t-test was used to identify areas of relative hypo and hypermetabolism in both CdC-patient group and single patient subjects. Age and gender were included as nuisance in all SPM analyses. We used a p value threshold of 0.05, corrected for multiple comparisons with the False Discovery Rate (FDR) option, to explore SPM t-maps at

the cluster and voxel level, considering as significant clusters with more than 100 voxels. If statistical significance was not reached the threshold at the voxel level was explored at $p<0.001$ uncorrected for multiple comparisons.

RESULTS

Patient Clinical Characteristics

According to the DSM V criteria, the subjects were classified with mild (2 patients; n. 4 and 6) and severe (4 patients: n, 1, 2, 3 5) clinical phenotype. Patient characteristics are summarized in Table 1. All patients with severe phenotype presented speaking and socialization problems. Impairment in the execution of daily activities was the most frequent clinical characteristic (3/4 patients with severe phenotype), along with microcephay (3/4 patients) and reduced pain sensibility (3/4 patients). Movement disorders were present in 3/4 patients with severe phenotype. Skin picking was documented in one patient with severe phenotype. A patients with mild phenotype presented socialization problems and movement disorders. Hashimoto's Thyroiditis was present in both the twin patients (patients n. 5 and 6, patient n. 5 with severe phenotype and the other one with mild phenotype).

Patient Genetic Abnormalities

Patients with severe phenotype presented the following genetic mutations: 46,XY,del(5)(p14.3->pter) present in two patients (n. 1 and 2); 46,XY,del(5)(p15.1->pter) in patient n. 3; 46,XY,ish del(5)(p14)/46,XY in patient n. 5. The genetic mutations in patients with mild phenotype were 46XX,del(5)(p15.2->pter) and 46,XY,ish del(5)(p14)/46,XY in patient n. 4 and in patient n. 6, respectively. The karyotype found in the twin patients (cases 5 and 6, one with severe phenotype and the other one with mild phenotype) was 46,XY,ish del (5)(p14).

SPM Analysis

SPM group analysis revealed a statistically significant relative hypometabolism in the left temporal lobe (BAs 20, 36 and 38) in the patient group compared to the control cohort ($p<0.001$). Furthermore, hypometabolism was also detected in the right frontal subcallosal gyrus (BA 34) and caudate body, and in the cerebellar tonsils (Figure 1; Table 2).

Statistically significant relative hypermetabolism ($p=0.001$) was found in the right premotor cortex (BA 6) in the patients group in comparison with the controls (Figure 1). In SPM single subject analysis the hypermetabolic areas were detected only in patients with a severe phenotype (Figure 2).

DISCUSSION

The diagnostic work-up of CdCs includes clinical assessment and genetic evaluation/examination to detect deletion of 5p. Brain MRI is used to uncover structural brain abnormalities, such as marked atrophy in the brainstem, small cerebellum and middle cerebellar peduncles (6, 7, *14, 15*).

To the best of our knowledge, the present study is the first report describing the use of ^{18}F-FDG-PET/CT in the evaluation of brain glucose metabolism in patients with CdCs. All patients demonstrated several hypometabolic brain areas at the SPM analysis. ^{18}F-FDG hypometabolism is a common feature in many neurological diseases (*16*) and characteristic spatial patterns have been identified in different neurological conditions, reflecting a number of possible causes, such as brain atrophy, decreased cerebral metabolic rate of glucose, regional synaptic dysfunction or deafferentation and transneural metabolic depression (*17-19*).

The main hypometabolic region detected in our patients was the left inferior temporal and homolateral temporal pole cortex (BAs 20, 34 36, 38) that are involved in verbal production and comprehension, working memory and selective attention to speech (*20-22*). Furthermore, the left BA 20 is involved in the process of language associations and perceptual skills (*20-23*), whereas the left BAs 34 and 36 are associated to the ability of experiencing and processing emotion; these areas also contribute to the novelty discrimination (*24,25*). Although the hypometabolism in these areas can be related to the cognition alterations and disturbances in emotion, memory and language in our CdC patients, (*26-29*), these defects are not sufficient alone to explain all the clinical features of patients with a severe phenotype. Interestingly, in our patients significant hypometabolism was also found in the cerebellar tonsils. These structures belong to the neocerebellum, which receives inputs from the cerebral cortex and helps in the planning of the movement of the distal portions of the limbs (*30*). The reduced glucose metabolism in cerebellar tonsils may reflect reduced inhibition of the circuits directed to the vestibular nuclei and contribute to explain the movement disorders documented in our patients. This hypothesis finds support in few studies reporting reduced glucose metabolism in cerebellar tonsils in congenital ocular motor apraxia (*31*) and downbeat nystagmus (*32*).

In the scarce available literature, vermian hypoplasia has been reported as a hallmark of patients with CdCs in MRI studies (*33*). However, in our study, we found only a trend to hypometabolism in this structure. We hypothesize that future larger studies, may be able to clarify the significance of this result.

The phenomenon of skin picking was documented only in one subject in our patient cohort (*34,35*). Vogt and coworkers evaluated the regional cerebral blood flow (rCBF) by means of $^{15}OH_2$ PET in 7 normal healthy subjects receiving neuropsychological and pain threshold testing (*36*). They documented a reduction of rCBF in 6/7 subjects in the BA 30 (in the right, left or both hemispheres) during noxiuous stimulation. In further two fMRI studies, a reduction of the signal in Bas 30 and 5 has been related to noxious stimuli *(37,38).* All this evidence suggests that the BAs 5 and 30 are involved in some aspects

of the pain experience. However, in our cohort, the only patient presenting skin picking did not show metabolic alterations in these areas, but he demonstrated hypometabolism in the right caudate body. This latter finding could be in keeping with that of previous researchers, who documented functional underactivation in bilateral striatum (maximal in right caudatum) in a small group of patients with excoriation (skin-picking) disorder (*39*). However, due to the limited number of patients of our study and lack of literature describing PET or fMRI findings in patients with CdCs with skin picking, it is not possible to make a definitive conclusions in this regard.

In our study, we could not establish whether patients with a mild phenotype presented less severe hypometabolism than patients with severe phenotype or vice versa due to the limited number of subjects in the two groups. Nevertheless, at the single subject analysis, the two patients with mild phenotype, despite presenting the same hypometabolic brain regions as patients with severe phenotype, did not show the same symptoms. The main differences between the two clinical phenotype of our study were related the hypermetabolic findings. Infact, hypermetabolic areas were not identified in patients with mild phenotype. The role of the ^{18}F-FDG hypermetabolic regions in the disease progression is unclear. ^{18}F-FDG hypermetabolism has been linked in other diseases, such as amyotrophic lateral sclerosis, to increased astrocytosis, an hallmark of microglial activation (*4*). However, no study has ever elucidated the association of microglia and disease expression in patients with CdCs. In our opinion, hypermetabolic alterations may play a role in determining the expression of phenotype since, in single subject analysis, patients without hypermetabolic abnormalities did no present severe clinical phenotype. In severe phenotype patients, the hypermetabolic alteration involved the right premotor cortex (BA 6). This alteration could be important to explain at least a part of movement symptoms because this region is connected with the spinal cord via the cortico-ponto-cerebellar pathway (*40*). The end point of future next study will be to establish the correlation between the hypermetabolic finding in premotor cortex and hypometabolic features in cerebellum in a more large population affected by Cri du Chat Syndrome. Limits of our study were the low number of patients due the relative rarity of the disease, the heterogeneous distribution of the genetic alterations within the patient group and the lack of morphological imaging exams, such as MRI, to compare ^{18}F-FDG uptake with anatomical alterations. Finally, part of the results could also be influenced by the heterogeneous age group of the patients, which may be linked to different stages of the behavioural, scholar and educational development. Future studies should try to collect larger number of patients to confirm the PET imaging findings presented in this study and, specifically, to confirm whether hypermetabolic alterations are the typical features of patients with severe phenotype.

CONCLUSION

Different brain glucose metabolic alterations can be identified by^{18}F-FDG PET/CT in Cri du Chat patients with severe and mild phenotype compared to control subjects. In particular, hypometabolic areas were found in left temporal lobe, right

frontal subcallosal gyrus, right caudate body and cerebellar tonsils bilaterally, whereas hypermetabolic findings were identified only in patients with severe phenotype. Further studies with more numerous patient cohorts are warranted to confirm these results and to evaluate the influence of different deletion sites of 5p in brain glucose metabolism.

DISCLOSURE

No actual or potential conflicts of interest exist. The publication of this study has been financially supported by ABC (Associazione Bambini Cri du Chat).

ACKNOWLEDGEMNTS

We thank the patients and parents for their collaboration in this study. A lovely thanks to Sylvia Teresa Del Testa for the special support for inspiring the start of the study.

KEY POINTS

QUESTION: Is brain metabolism altered in patients with Cri Du Chat Syndrome with mild and severe phenotype?

PERTINENT FINDINGS: In a small cohort of 6 patients, significant hypometabolism ($p<0.001$) was found using ^{18}F-FDG PET imaging in the left temporal lobe (BAs 20, 36 and 38), right frontal subcallosal gyrus (BA 34), right caudate body and in the cerebellar tonsils. Significant hypermetabolism ($p=0.001$) was detected in patients with severe phenotype in the right superior and precentral frontal gyrus (BA 6).

IMPLICATIONS FOR PATIENT CARE: ^{18}F-FDG PET imaging may highlight altered brain metabolism in patients with Cri Du Chat Syndrome and help differentiate severe from mild phenotype.

REFERENCES

1. Cerruti Mainardi P. Cri du Chat syndrome. *Orphanet J Rare Dis.* 2006;1:33.
2. Guala A, Spunton M, Tognon F, et al. Psychomotor development in Cri du Chat syndrome: comparison in two Italian cohorts with different rehabilitation methods. *ScientificWorldJournal.* 2016;2016:3125283.
3. Mainardi PC, Perfumo C, Calì A, et al. Clinical and molecular characterisation of 80 patients with 5p deletion: genotype-phenotype correlation. *J Med Genet.* 2001;38:151-158.
4. Nguyen JM, Qualmann KJ, Okashah R, Reilly A, Alexeyev MF, Campbell DJ. 5p deletions: current knowledge and future directions. *Am J Med Genet C Semin Med Genet.* 2015;169:224-238.
5. Correa T, Feltes BC, Riegel M. Integrated analysis of the critical region 5p15.3-p15.2 associated with cri-du-chat syndrome. *Genet Mol Biol.* 2019;42:186-196.
6. Nandhagopal R, Udayakumar AM. Cri-du-chat syndrome. *Indian J Med Res.* 2014;140:570-571.
7. Hong JH, Lee HY, Lim MK, et al. Brain stem hypoplasia associated with Cri-du-Chat syndrome. *Korean J Radiol.* 2013;14:960-962.
8. Cistaro A, Caobelli F, Quartuccio N, Fania P, Pagani M. Uncommon 18F-FDG-PET/CT findings in patients affected by limbic encephalitis: hyper-hypometabolic pattern with double antibody positivity and migrating foci of hypermetabolism. *Clin Imaging.* 2015;39:329-333.
9. Cistaro A, Cuccurullo V, Quartuccio N, Pagani M, Valentini MC, Mansi L. Role of PET and SPECT in the study of amyotrophic lateral sclerosis. *Biomed Res Int.* 2014;2014:237437.
10. Politis M, Piccini P. Positron emission tomography imaging in neurological disorders. *J Neurol.* 2012;259:1769-1780.
11. Vahia VN. Diagnostic and statistical manual of mental disorders 5: a quick glance. *Indian J Psychiatry.* 2013;55:220-223.
12. Varrone A, Asenbaum S, Vander Borght T, et al. EANM procedure guidelines for PET brain imaging using [18F]FDG, version 2. *Eur J Nucl Med Mol Imaging.* 2009;36:2103-2110.
13. Cistaro A, Valentini MC, Chio A, et al. Brain hypermetabolism in amyotrophic lateral sclerosis: a FDG PET study in ALS of spinal and bulbar onset. *Eur J Nucl Med Mol Imaging.* 2012;39:251-259.
14. Tamraz J, Rethore MO, Lejeune J, et al. Brain morphometry using MRI in Cri-du-Chat Syndrome. Report of seven cases with review of the literature. *Ann Genet.* 1993;36:75-87.
15. De Michele G, Presta M, Di Salle F, et al. Cerebellar vermis hypoplasia in a case of cri-du-chat syndrome. *Acta Neurol (Napoli).* 1993;15:92-96.
16. Zilberter Y, Zilberter M. The vicious circle of hypometabolism in neurodegenerative diseases: ways and mechanisms of metabolic correction. *J Neurosci Res.* 2017;95:2217-2235.
17. Agrawal KL, Mittal BR, Bhattacharya A, Khandelwal N, Prabhakar S. Crossed cerebellar diaschisis on F-18 FDG PET/CT. *Indian J Nucl Med.* 2011;26:102-103.
18. Berti V, Mosconi L, Pupi A. Brain: normal variations and benign findings in fluorodeoxyglucose-PET/computed tomography imaging. *PET clin.* 2014;9:129-140.
19. Shivamurthy VK, Tahari AK, Marcus C, Subramaniam RM. Brain FDG PET and the diagnosis of dementia. *AJR Am J Roentgenol.* 2015;204:W76-85.
20. Ardila A, Bernal B, Rosselli M. How localized are language brain areas? A review of Brodmann areas involvement in oral language. *Arch Clin Neuropsychol.* 2016;31:112-122.
21. Papathanassiou D, Etard O, Mellet E, Zago L, Mazoyer B, Tzourio-Mazoyer N. A common language network for comprehension and production: a contribution to the definition of language epicenters with PET. *Neuroimage.* 2000;11:347-357.
22. Yoo SS, Paralkar G, Panych LP. Neural substrates associated with the concurrent performance of dual working memory tasks. *Int J Neurosci.* 2004;114:613-631.
23. Perobelli S, Alessandrini F, Zoccatelli G, et al. Diffuse alterations in grey and white matter associated with cognitive impairment in Shwachman-Diamond syndrome: evidence from a multimodal approach. *Neuroimage Clin.* 2015;7:721-731.
24. Habib R, McIntosh AR, Wheeler MA, Tulving E. Memory encoding and hippocampally-based novelty/familiarity discrimination networks. *Neuropsychologia.* 2003;41:271-279.
25. Vorobyev VA, Alho K, Medvedev SV, et al. Linguistic processing in visual and modality-nonspecific brain areas: PET recordings during selective attention. *Brain Res Cogn Brain Res.* 2004;20:309-322.
26. Hermann BP, Wyler AR, Richey ET, Rea JM. Memory function and verbal learning ability in patients with complex partial seizures of temporal lobe origin. *Epilepsia.* 1987;28:547-554.
27. Hoon Jr. AH, Reiss Jr. AL. The mesial-temporal lobe and autism: case report and review. *Dev Med Child Neurol.* 1992;34:252-259.
28. Lansdell H. Effect of extent of temporal lobe ablations on two lateralized deficits. *Physiol Behav.* 1968;3:271-273.
29. Lee TMC, Yip JTH, Jones-Gotman M. Memory deficits after resection from left or right anterior temporal lobe in humans: a meta-analytic review. *Epilepsia.* 2002;43:283-291.
30. Mavridis I. Gross and neurosurgical anatomy of the cerebellar tonsil. *OA Anatomy.* 2014;2:8.
31. Jang SJ, Kim YK, Oh YM, Kim JS, Lee WW, Kim SE. Cerebellar vermian hypometabolism in children with congenital ocular motor apraxia [abstract]. *J Nucl Med.* 2007;48(suppl 2):171 P.

32. Bense S, Best C, Buchholz HG, et al. 18F-fluorodeoxyglucose hypometabolism in cerebellar tonsil and flocculus in downbeat nystagmus. *Neuroreport.* 2006;17:599-603.
33. Rolls ET, Grabenhorst F. The orbitofrontal cortex and beyond: from affect to decision-making. *Prog Neurobiol.* 2008;86:216-244.
34. Spunton M, Guala A, Liverani ME, et al. Skin picking disorder in 97 Italian and Spanish Cri du chat patients. *Am J Med Genet A.* 2019;179:1525-1530.
35. Fergnani VGC, Guala A, Danesino C, et al. Genetic and neuroradiological clinical correlations in Cri Du Chat syndrome. Paper presented at: ESHG, European Human Genetics Conference 16-19 June 2018, 2018; Milan.
36. Vogt BA, Derbyshire S, Jones AK. Pain processing in four regions of human cingulate cortex localized with co-registered PET and MR imaging. *Eur J Neurosci.* 1996;8:1461-1473.
37. Kong J, Loggia ML, Zyloney C, Tu P, Laviolette P, Gollub RL. Exploring the brain in pain: activations, deactivations and their relation. *Pain.* 2010;148:257-267.
38. Apkarian AV, Darbar A, Krauss BR, Gelnar PA, Szeverenyi NM. Differentiating cortical areas related to pain perception from stimulus identification: temporal analysis of fMRI activity. *J Neurophysiol.* 1999;81:2956-2963.
39. Odlaug BL, Hampshire A, Chamberlain SR, Grant JE. Abnormal brain activation in excoriation (skin-picking) disorder: evidence from an executive planning fMRI study. *Br J Psychiatry.* 2016;208:168-174.
40. Palesi F, De Rinaldis A, Castellazzi G, et al. Contralateral cortico-ponto-cerebellar pathways reconstruction in humans in vivo: implications for reciprocal cerebro-cerebellar structural connectivity in motor and non-motor areas. *Sci Rep.* 2017;7:12841.

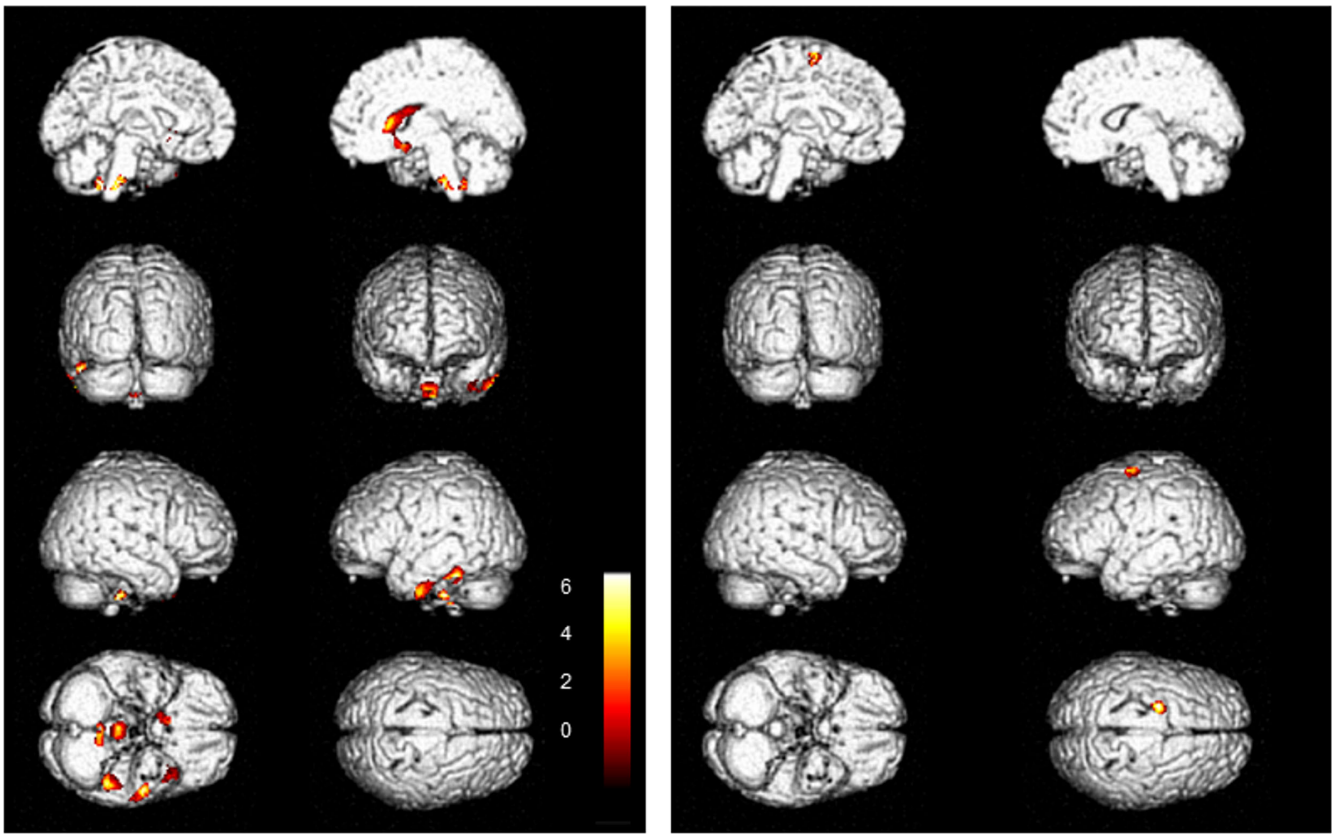

FIGURE 1 PET imaging. Brain three-dimensional rendering showing those regions in which ^{18}F-FDG uptake was significantly different in CdCs patients (n=6) than in the controls (threshold $p<0.001$, uncorrected for multiple comparisons at voxel level): top row left medial left view; top row right medial right view; second row left posterior view; second row right frontal view; third row left right-side view; third row right left-side view; bottom row left view from below; bottom row right view from above. Images are color-graded in terms of z values. Left image: Controls *vs.* patient group. Relative hypometabolism in the left temporal lobe (Brodmann areas 20, 36 and 38). Right image: patient group *vs.* controls. Relative hypermetabolism in the right middle frontal gyrus (Broadmann area 6.) Talairach coordinate and regional details are provided in Table 2.

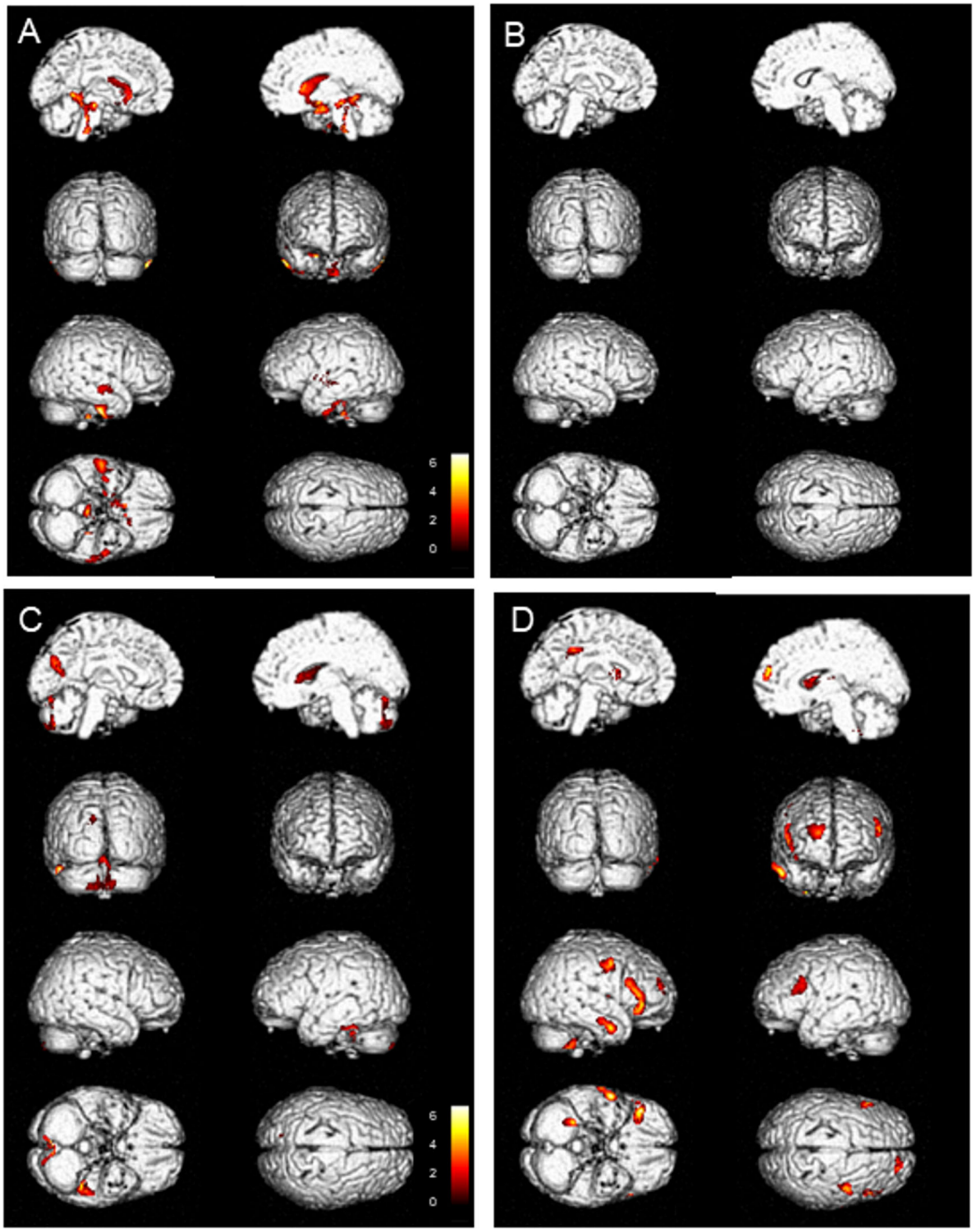

FIGURE 2. PET imaging. Brain three-dimensional rendering showing those regions in which ^{18}F-FDG uptake was significantly different in the single patient with CdC compared to the normal database (threshold $p<0.001$, uncorrected for multiple comparisons at voxel level). Images are color-graded in terms of z values. Top images: Relative hypo- (A) and hypermetabolism (B) in a patient with mild phenotype. Botton images: Relative hypo- (C) and hypermetabolism (C) in a patient with severe phenotype. Of note, the patient with mild phenotype does not show any hypermetabolic finding (B and D).

Pt.	Age	Sex	Ph.	Clinical symptoms										
				Mental disability	Reading problems	Speaking problems	Movement disorders	Dyspraxia	Aggressive behavior	Difficulties in daily activities	Socialization problems	Microcephaly	Reduced pain sensibility	Skin picking
1	26	M	severe	severe	-	+	+	+	+	+	+	+	+	-
2	23	M	severe	severe	+	+	+	+	+	+	+	+	+	+
3	27	M	severe	moderate	-	+	-	+	-	-	+	-	+	-
4	10	F	mild	mild	-	-	+	-	-	-	+	-	-	-
5	15	M	severe	severe	+	+	+	+	-	+	+	+	-	-
6	15	M	mild	mild	-	-	-	-	-	-	-	-	-	-

TABLE 1 Summary of patient characteristics with main clinical manifestations. Case 5 and 6 are monozygotic twins; mosaic were studied in peripheral lymphocytes. Ph.= phenotype; **+** = presence; - = absence.

	Cluster-level		**Peak-level**						
contrast	K extantion	p uncorr	Z	X coor	Y coor	Z coor	Level 1	Level 3	Level 5
CONTROL - CRI GROUP 0.001	361	0,001	5.03	18.0	20.0	6.0	Right Cerebrum	Caudate	Caudate Body
				16.0	3.0	-12.0	Right Cerebrum	Subcallosal Gyrus	Brodmann area 34
	226	0,004	4.85	-46.0	-40.0	-20.0	Left Cerebrum	Fusiform Gyrus	Brodmann area 36
	204	0,006	4.52	-53.0	-12.0	-36.0	Left Cerebrum	Inferior Temporal Gyrus	Brodmann area 20
				-59.0	-17.0	-28.0	Left Cerebrum	Fusiform Gyrus	Brodmann area 20
	155	0,014	3.96	-10.0	-49.0	-38.0	Left Cerebellum	Cerebellar Tonsil	*
				2.0	-47.0	-40.0	Right Cerebellum	Cerebellar Tonsil	*
	117	0,029	3.83	-36.0	17.0	-36.0	Left Cerebrum	Superior Temporal Gyrus	Brodmann area 38
				-42.0	9.0	-41.0	Left Cerebrum	Middle Temporal Gyrus	Brodmann area 38
CRI GROUP – CONTROL 0.001	111	0,033	4.06	-20.0	-1.0	59.0	Left Cerebrum	Middle Frontal Gyrus	Brodmann area 6

TABLE 2 Talairach coordinate and regional details. Threshold $p<0.001$, uncorrected at voxel level. A value of ≤ 0.05, corrected for multiple comparison at the cluster level, was accepted as statistically significant. The corresponding cortical region and BA are reported for each significant cluster. If the maximum correlation is achieved outside the grey matter, the nearest grey matter (within a range of 3 mm) is indicated with the corresponding BA.